

Published in final edited form as:

Nat Med. ; 18(4): 595–599. doi:10.1038/nm.2710.

Genetically determined P2X7 receptor pore formation regulates variability in chronic pain sensitivity

Robert E Sorge^{1,14}, Tuan Trang^{2,14}, Ruslan Dorfman², Shad B Smith^{3,4}, Simon Beggs², Jennifer Ritchie¹, Jean-Sebastien Austin¹, Dmitri V Zaykin⁵, Heather Vander Meulen², Michael Costigan⁶, Teri A Herbert⁶, Merav Yarkoni-Abitbul⁷, David Tichauer⁷, Jessica Livneh⁸, Edith Gershon⁹, Ming Zheng¹⁰, Keith Tan¹¹, Sally L John¹¹, Gary D Slade^{4,12}, Joanne Jordan¹³, Clifford J Woolf⁶, Gary Peltz¹⁰, William Maixner^{3,4}, Luda Diatchenko^{3,4}, Ze'ev Seltzer⁷, Michael W Salter^{2,7}, and Jeffrey S Mogil^{1,4}

¹Department of Psychology and Alan Edwards Centre for Research on Pain, McGill University, Montreal, Quebec, Canada

²Program in Neurosciences & Mental Health Hospital for Sick Children, Toronto, Ontario, Canada

³Center for Neurosensory Disorders, University of North Carolina at Chapel Hill, Chapel Hill, North Carolina, USA

⁴Algynomics Inc., Chapel Hill, North Carolina, USA

⁵National Institute of Environmental Health Sciences, National Institutes of Health, Research Triangle Park, North Carolina, USA

⁶Department of Neurobiology, Harvard Medical School, Boston, Massachusetts, USA

⁷Faculties of Dentistry and of Medicine, University of Toronto, Toronto, Ontario, Canada

⁸Oncology Institute, Sheba Medical Centre, Ramat Gan, Israel

⁹Ein Hod, Hof Hacarmel, Israel

¹⁰Department of Anesthesia, Stanford University School of Medicine, Stanford, California, USA

¹¹Pfizer Global Research and Development, Sandwich, UK

¹²Department of Dental Ecology, School of Dentistry, University of North Carolina at Chapel Hill, Chapel Hill, North Carolina, USA

¹³Thurston Arthritis Center, University of North Carolina at Chapel Hill, Chapel Hill, North Carolina USA

Abstract

Chronic pain is highly variable between individuals, as is the response to analgesics. Although much of the variability in chronic pain and analgesic response is heritable, an understanding of the

Correspondence should be addressed to J.S.M. (jeffrey.mogil@mcgill.ca) or M.W.S. (mike.salter@utoronto.ca).

¹⁴These authors contributed equally to this work.

Author Contributions: R.E.S., T.T., R.D., S.B.S., S.B., J.R., J.-S.A., D.V.Z., H.V.M., M.C., T.A.H., M.Y.-A., D.T., E.G., M.Z., J.L. and G.P. generated data, performed analyses or both. R.E.S., S.B., C.J.W., W.M., L.D., Z.S., K.T., G.D.S., J.J., S.L.J., T.T., M.W.S. and J.S.M. contributed to the design of the study and supervised the analyses. R.E.S., T.T., M.W.S. and J.S.M. wrote the manuscript. All authors read and approved the final manuscript.

Competing Financial Interests: The authors declare competing financial interests: details accompany the full-text HTML version of the paper at <http://www.nature.com/naturemedicine/>.

Note: Supplementary information is available on the Nature Medicine website.

genetic determinants underlying this variability is rudimentary¹. Here we show that variation within the coding sequence of the gene encoding the P2X7 receptor (P2X7R) affects chronic pain sensitivity in both mice and humans. P2X7Rs, which are members of the family of ionotropic ATP-gated receptors, have two distinct modes of function: they can function through their intrinsic cationic channel or by forming nonselective pores that are permeable to molecules with a mass of up to 900 Da^{2,3}. Using genome-wide linkage analyses, we discovered an association between nerve-injury-induced pain behavior (mechanical allodynia) and the P451L mutation of the mouse *P2rx7* gene, such that mice in which P2X7Rs have impaired pore formation as a result of this mutation showed less allodynia than mice with the pore-forming *P2rx7* allele. Administration of a peptide corresponding to the P2X7R C-terminal domain, which blocked pore formation but not cation channel activity, selectively reduced nerve injury and inflammatory allodynia only in mice with the pore-forming *P2rx7* allele. Moreover, in two independent human chronic pain cohorts, a cohort with pain after mastectomy and a cohort with osteoarthritis, we observed a genetic association between lower pain intensity and the hypofunctional His270 (rs7958311) allele of *P2RX7*. Our findings suggest that selectively targeting P2X7R pore formation may be a new strategy for individualizing the treatment of chronic pain.

To identify genetic determinants of variability in mechanical allodynia, which is a major symptom of chronic pain, we performed an unbiased genome-wide screen in mice. We assessed the severity of abnormal tactile hypersensitivity in 18 inbred mouse strains of diverse genetic backgrounds after spared nerve injury (SNI) and found robust inter-strain differences in tactile hypersensitivity in these mice (Fig. 1a). We found the main effects of strain (genotype), repeated measures and their interaction on ipsilateral hindpaw withdrawal thresholds to von Frey filament stimulation to be highly significant (all $P < 0.001$; Supplementary Fig. 1). After z-score transformation of the strain means (Fig. 1b), we analyzed the standardized data using a haplotype-based computational genetic mapping method, which identifies genomic regions where the pattern of sequence variation across strains within a haplotype block correlates with the variation in the amount of allodynia across the analyzed strains⁴. A number of genomic regions were highly correlated with the standardized strain means (Supplementary Table 1), but we focused here on the haplotype block with the strongest correlation genome wide, which was within the *P2rx7* gene ($P = 0.00056$; Fig. 1c). This haplotype block, spanning ~8 kb and located between 123.124–123.132 Mb on chromosome 5, contains 24 single nucleotide polymorphisms (SNPs) and forms two contrasting haplotypes in the set of 18 strains (Supplementary Fig. 2).

The only nonsynonymous SNP (rs48804829; T1352C) in this block produces a proline to leucine change at amino acid 451 (P451L) of the P2X7R (located in the cytoplasmic domain of P2X7R); this mutation is known to affect pore formation in cell membranes⁵. Therefore, we hypothesized that P451L genotype (that is, whether the Pro451 allele or the Leu451 allele was present) might affect allodynia severity. Consistent with this genetic hypothesis, six of the seven mouse strains with less than average allodynia carried the Leu451 allele (Fig. 1b). Overall, P451L genotype had no effect on mechanical nociceptive sensitivity in naive, noninjured mice ($t_{16} = 0.2$; Fig. 1d), but it robustly affected mechanical allodynia severity in mice with SNI ($t_{16} = 4.3$, $P < 0.001$; Fig. 1e), accounting for 16.1% of the trait variance and a full 50% of the genetic variance across all strains. Changes on the contralateral hindpaw were also dependent on P451L status ($t_{16} = 2.2$, $P < 0.05$; Fig. 1f); only the strains with the Leu451 allele had significant ($t_{40} = 2.7$, $P < 0.005$) hypoalgesia. To provide an independent assessment of the genetic effect of P451L genotype, we examined SNI-induced mechanical allodynia in a second set of 15 mouse strains, which were tested in a different laboratory (Fig. 1g and Supplementary Fig. 3). Strains carrying the Leu451 allele had significantly lower allodynia in this validation cohort than did those strains carrying the Pro451 allele ($t_{13} = 3.1$, $P < 0.01$).

To investigate the mechanism of the P451L allelic effect on allo-dynia, we characterized P2X7R function in two representative mouse strains, one carrying the Pro451 variant (A/J) and the other carrying the Leu451 allele (B10.D2). We assessed both the function of the P2X7R to open pores that are permeable to molecules up to ss900 Da and the function of the receptor as a nonselective cation channel^{2,3}. To assess pore formation, we loaded peritoneal macrophages with the acetomethoxy derivate of calcein (calcein AM) and exposed them to a P2X7R agonist, 3'-O-(4-benzoyl)benzoyl adenosine 5'-triphosphate (BzATP, 300 μ M). We found that exposure to BzATP caused a loss of calcein in macrophages from A/J mice but not in those from B10.D2 mice (Fig. 2a–c). We therefore examined whether this difference in pore formation was specifically the result of an allelic difference within the P2X7Rs of these two strains. The BzATP-induced loss of calcein in the A/J macrophages was blocked by the P2X7R antagonist Brilliant Blue G (BBG, 1 μ M; Fig. 2d) and was prevented by the pannexin 1 inhibitors ¹⁰Panx (300 μ M; Fig. 2e) and carbenoxolone (10 μ M; Fig. 2f); this response was unaffected by a scrambled, inactive version of ¹⁰Panx, scr Panx (300 μ M; Fig. 2f). The expression of P2X7R (Fig. 2g) or pannexin 1 protein (data not shown) did not differ between B10.D2 and A/J mice. Moreover, exposure to BzATP induced a rapid rise in intracellular Ca²⁺ concentration in B10.D2 macrophages that was indistinguishable from that in A/J macrophages (Fig. 2h). The BzATP-induced rise in intracellular [Ca²⁺] occurred before the start of the calcein loss and was blocked by BBG but was unaffected by ¹⁰Panx, scr Panx or carbenoxolone (Fig. 2i). Together, these findings show that whereas functional P2X7Rs are expressed in both mouse strains, P2X7R activation leads to pore formation through coupling to pannexin 1 channels in A/J but not B10.D2 mice.

To target the P451L site that differentiates the P2X7Rs of these two strains, we used a peptide (TAT-P451) comprised of the sequence of amino acids 445–455 of the P2X7R of the Pro451 isoform fused to the 11-amino-acid protein transduction domain of the human immuno-deficiency virus 1 (HIV-1) TAT protein, which blocks P2X7R-mediated pore formation in J774 cells⁶. We fused the corresponding sequence of the Leu451 isoform of the peptide, which is inactive⁶, with the TAT sequence (TAT-451L) and used this as a negative control. We found that the TAT-P451 peptide, but not the TAT-451L version, prevented (Fig. 3a–c) or reversed (Fig. 3d) the pore formation induced by administering BzATP to A/J macrophages. By contrast, neither TAT-P451 nor TAT-451L affected the nonselective cation channel function of the P2X7Rs in macrophages from A/J (Fig. 3e,f) or B10.D2 mice (Fig. 3f). Thus, TAT-P451 differentially blocks P2X7R-mediated pore formation in A/J mice but does not affect P2X7R channel function in either A/J or B10.D2 mice. We therefore examined whether TAT-P451 affects allodynia in a strain-dependent or a strain-independent manner. We found that intravenous administration of TAT-P451 reversed the mechanical allodynia induced by SNI in A/J mice but that it had no effect in B10.D2 mice (Fig. 3g and Supplementary Fig. 4). Similarly, TAT-P451 attenuated the mechanical allodynia caused by hindpaw injection of the inflammatory agent complete Freund's adjuvant (CFA) in A/J but not B10.D2 mice (Fig. 3h and Supplementary Fig. 4). TAT-451L had no effect in either strain on the mechanical allodynia evoked by SNI or CFA. Thus, mechanical allodynia caused by either peripheral nerve injury or inflammation is differentially blocked by TAT-P451 in mice expressing the pore-forming isoform but not in those expressing the non-pore-forming isoform of P2X7R. That a gene identified by screening for neuropathic pain in mice would also be relevant to inflammatory pain is not unexpected based on previous observations of high genetic correlations of pain symptoms in mouse strains across differing etiologies⁷.

In humans, the *P2RX7* gene is highly polymorphic⁸, and genetic differences within *P2RX7* affect P2X7R pore formation and channel function, which may contribute to variability in chronic pain sensitivity. To test whether pain sensitivity is associated with variations in *P2RX7*, we genotyped 30 haplotype-tagging SNPs in a retrospectively collected cohort of

354 women who underwent breast surgery to remove a malignant tumor complemented by axillary lymph node resection. About half of these women developed chronic pain after their mastectomy (post-mastectomy pain, PMP). Three SNPs, two of which are known functional missense variants affecting P2X7R pore formation, showed a significant ($0.003 < P < 0.006$) association with the ratings of intensity of a typical pain episode in these patients (Fig. 4 and Supplementary Table 2). Women carrying the Tyr155 allele at rs208294 (H155Y)—previously shown in human macrophages to be a hyperfunctional variant⁹—reported higher amounts of pain than did carriers of the His155 allele. Conversely, carriers of the His270 allele at rs7958311 (R270H), which is hypofunctional compared to the Arg270 allele¹⁰ (Supplementary Fig. 5), reported lower amounts of pain than did carriers of the Arg270 allele. Because the SNP associations revealed two missense variants with opposing functional consequences and one variant with an unknown effect (the intronic SNP rs208296), we combined these three SNPs into a haplotype explaining 4.5% of the trait variance seen in these patients, which delineated the differential effects of these variants on PMP and decreased the association *P* values ($P = 0.001$) that were compatible with the mixed effects these alleles had in the various haplotypes (Supplementary Table 3).

To determine whether there was an association between *P2RX7* genotype and the amounts of pain in an independent chronic pain cohort, we examined the same three SNPs in 743 patients suffering from osteoarthritis, a chronic inflammatory disease with a substantial pain burden that is highly variable between individuals, compared to 586 unaffected controls. Genotypic association analyses in this cohort showed an association of the rs7958311 SNP with the risk of having clinically relevant pain (defined as a score ≥ 3 on the Western Ontario and McMaster Universities Osteoarthritis Index (WOMAC) pain sub-scale; $P = 0.015$) (Fig. 4 and Supplementary Table 2). Again, we found highly significant associations for the haplotypes of these SNPs with pain (Supplementary Table 3). Although the significant associations present in this cohort were for haplotypes that differed from those that were significant in the PMP cohort, the direction of the effect exerted by these haplotypes (accounting for $\sim 1\%$ of the trait variance) was compatible with the direction observed for the PMP cohort.

To determine whether there was concordance of this genetic association, we carried out a meta-analysis combining the data from the PMP and osteoarthritis cohorts for the 23 SNPs genotyped commonly in both cohorts using the optimally weighted *z*-test method¹¹. This analysis showed a significant association between the pore-disabling missense SNP rs7958311 and reduced amounts of chronic pain ($P = 3.3 \times 10^{-4}$; Fig. 4). These results confirmed that the hypofunctional His270 allele confers a protective effect for chronic pain susceptibility in humans, just as the pore-disabling Leu451 allele does in mice.

In summary, we have discovered that genetic variability in pore formation by P2X7Rs is a key determinant of the differences in experimentally induced pain in mice and in chronic pain conditions in humans. A role for P2X7Rs in chronic pain behaviors has been suggested based on the reduced pain sensitivity in P2X7R-null mutant mice^{12,13} and after pharmacological blockade of P2X7R^{14–17}. However, as cation channel function and pore formation were both impaired in these previous studies, it was unclear which of these two P2X7R functions is crucial to pain processing. Here, genetic and pharmacological evidence in mice and humans converged to indicate that it is P2X7R pore formation that is key in chronic pain. Our finding that blocking P2X7R pore formation reversed mechanical allodynia induced by SNI or by CFA indicates that pain hypersensitivity requires ongoing P2X7R pore formation. P2X7R-induced pore formation initiates numerous downstream effects that may mediate pain hypersensitivity, including the release of molecules such as interleukin-1 β and ATP^{18–20} from microglia or macrophages.

The identification of a protective *P2RX7* haplotype has potentially crucial implications for the prediction of an individual's risk of developing chronic pain and for individualizing the treatment of chronic pain. From our findings, we anticipate that individuals with pore-impaired P2X7Rs would be resistant to pharmacological interventions aimed at this target and, therefore, should not be subjected to such treatments. The use of *P2RX7* genotyping, or functionally assessed pore formation, to guide therapy may improve the outcomes of pain treatment and avoid exposing individuals to a therapy from which they are unlikely to benefit. However, specifically targeting P2X7R pore formation while leaving cation channel activity intact using molecules that act in a similar way to TAT-P451 could provide a preferred strategy for reducing pain in individuals who carry *P2RX7* haplotypes that confer a high risk for chronic pain. This approach would enable some P2X7R function to be retained while reducing the risk of side effects that could emerge from inhibiting both functions of this receptor.

Online Methods

Mice

Mice in the 18-strain survey were naive, adult inbred mice of both sexes²¹. Interim findings from the dataset described herein have been previously published²². The mice in the follow-up pharmacological experiments were naive, adult (7–12 weeks of age) outbred CD-1 (ICR:Cr1) mice of both sexes bred in our laboratory from mice obtained from Charles River (Boucherville, Quebec) or were A/J and B10.D2-H2/oSnJ (B10.D2) mice obtained from The Jackson Laboratory.

von Frey testing

The up-down method of Dixon²³ was used to estimate 50% withdrawal thresholds. In later experiments, an automated von Frey test (UgoBasile Dynamic Plantar Aesthesiometer) was used. Mice were only tested when alert or resting, not when grooming²⁴. At each time point, three separate threshold determinations were made on each hindpaw, and then the measurements were averaged.

SNI

All mice received unilateral SNI²⁵ (as adapted for mice²⁶) under isoflurane and oxygen anesthesia. von Frey fibers were applied to the lateral aspect of the plantar hindpaw to measure mechanical sensitivity at baseline (1 and 2 weeks before surgery) and on postoperative days 1, 4, 7, 14, 21 and 28. In the replication cohort, mice were retested on postoperative days 5 and 7.

CFA

Mice were given unilateral injections of CFA (50%, in a 20- μ l injection volume) and tested for mechanical sensitivity (using von Frey fibers, see above) at baseline and at 24 h and 48 h after injection to detect mechanical allodynia.

Haplotype mapping

The computational genetic analysis of the inbred strain data was performed using HapMapper, as previously described^{27,28}. A total of 5,694 haplotype blocks were generated from 215,155 SNPs characterized across all 18 inbred strains (www.ncbi.nlm.nih.gov/projects/SNP/).

Calcein dye loss and YO-PRO dye uptake assays for P2X7R-mediated pore formation

Cells were incubated with calcein AM (2.5 μ M; Invitrogen) or YO-PRO dye (2.5 μ M; Invitrogen) in extracellular recording solution (ECS) containing (in mM) NaCl 140, KCl 5.4, CaCl₂ 1.3, HEPES 10, glucose 33, pH 7.35, osmolality 315-320 mOsm. Experiments were performed at room temperature (20–22°C), and all drugs were applied in ECS. To initiate P2X7R pore formation, cells were stimulated with BzATP (300 μ M). Measurement of calcein fluorescence was performed by single-photon counting from individual macrophages using a photomultiplier detector. Measurement of YO-PRO fluorescence was performed using a fluorescence plate reader (Molecular Devices).

Fluorescent measurement of intracellular Ca²⁺ concentration

Peritoneal macrophages were incubated with the fluorescent Ca²⁺ indicator dye fura-2 AM (2.5 μ M; Molecular Probes) in ECS. As previously described in detail²⁹, after fluorophore loading, the cells were mounted on an inverted microscope (Diaphot-TMD, Nikon), and the 340 nm:380 nm fluorescence ratio was calculated after baseline subtraction.

In vitro pharmacology

For the calcein dye efflux, YO-PRO uptake and fluorescent measurement of intracellular Ca²⁺ experiments, drugs were applied by bath in ECS. Cells were stimulated with BzATP (300 μ M; Sigma). To block P2X7Rs, cells were pretreated with BBG (1 μ M; Sigma), an antagonist of P2X7Rs³⁰. To block P2X7R pore formation, we used the pannexin 1 inhibitor carbenoxolone (10 μ M) or ¹⁰Panx (300 μ M) and the scrambled inactive version of ¹⁰Panx, scr Panx (300 μ M). We also used a membrane-permeant fusion peptide (TAT-P451) comprised of the 11-amino-acid protein transduction domain of the HIV-1 TAT protein fused to 11 amino acids corresponding to the region 445–455 of P2X7R: SLHDSPPTPGQGGGYGRKKRRQRRR. The control peptide, TAT-451L, possessed an identical amino acid composition but had a leucine substitution: SLHDSPLTPGQGGGYGRKKRRQRRR.

In vivo pharmacology

We investigated the ability of BBG to both prevent the development of allodynia after nerve or inflammatory injury and reverse this allodynia once it had developed (Supplementary Fig. 6). We then investigated the ability of the two TAT fusion peptides (see above) to reverse neuropathic (SNI) and inflammatory (CFA) allodynia. The experimenters were blinded to the drug being administered.

Human pain cohorts

Two existing cohorts of human patients with chronic pain were genotyped as described below.

PMP cohort—The PMP cohort included 354 female patients. Because of the episodic nature of chronic pain in these patients, the pain intensity outcome was the intensity of a typical pain episode.

Osteoarthritis cohort—The osteoarthritis sample (743 cases and 586 controls) included participants of both sexes. The severity of pain in the patients with osteoarthritis was assessed using the pain subscale of the WOMAC 3.1 (Knee and Hip Osteoarthritis) index (<http://www.auscan.org/womac/>).

Genotyping

In both cohorts, DNA was extracted from whole-blood samples. The human *P2RX7* gene was genotyped using 23 tagging SNPs to cover the coding and noncoding parts of the gene and the 15-kb flanking regions. In the PMP cohort, genotyping of selected tagging SNPs (Fig. 4) was performed using the iPLEX Gold Sequenom platform at the Analytical Genetics Technology Centre, Princess Margaret Hospital, Toronto. In the osteoarthritis cohort, DNA was amplified and hybridized to Infinium 1M-Duo bead arrays (Illumina) according to Illumina standard procedures by Expression Analysis (Durham, NC).

Additional methods

Detailed methodology is described in the Supplementary Methods.

Supplementary Material

Refer to Web version on PubMed Central for supplementary material.

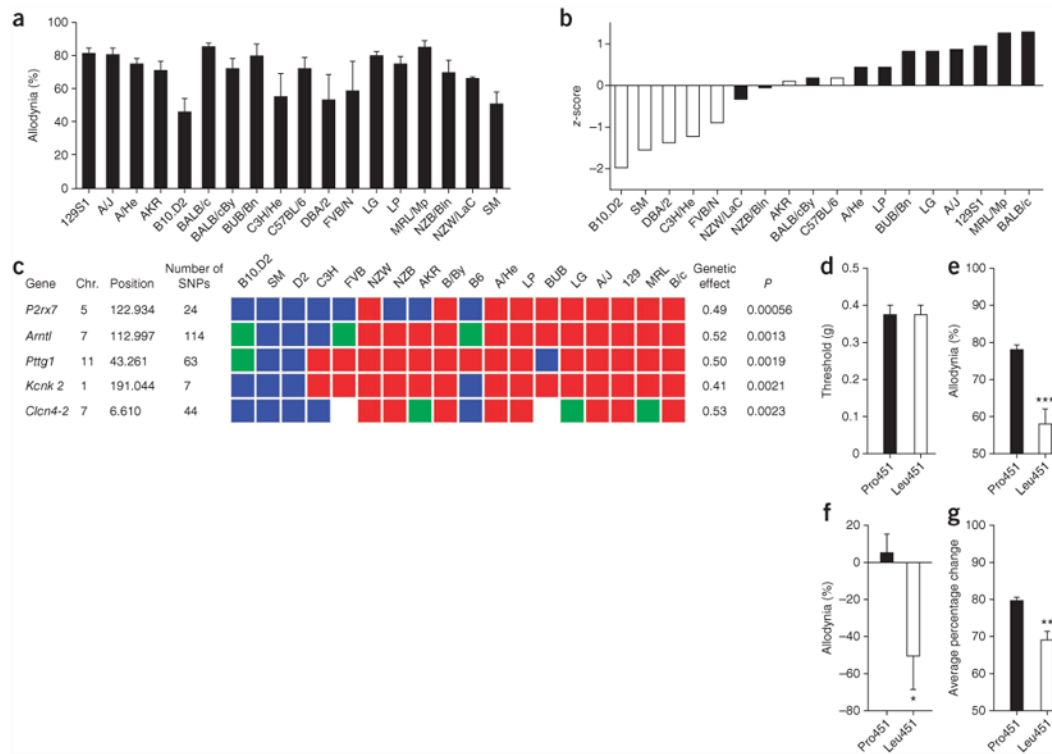
Acknowledgments

This research was supported by the US National Institutes of Health (NIH) (C.J.W., W.M., L.D., Z.S. and J.S.M.), the Louise and Alan Edwards Foundation (J.S.M.), the Canada Research Chairs program (M.W.S., J.S.M. and Z.S.), the Howard Hughes Medical Institute (M.W.S.), the Canadian Institutes of Health Research (M.W.S. and J.S.M.), the Krembil Foundation (M.W.S. and J.S.M.), the Ontario Research Foundation (M.W.S.) and Algyonics/Pfizer research funds (W.M., L.D.). R.E.S. was supported by an AstraZeneca–Alan Edwards Centre for Research on Pain postdoctoral fellowship. T.T. was supported by a Canadian Institutes of Health Research Fellowship. S.B.S. was supported by a National Research Service Award Fellowship from the NIH. D.V.Z. was supported by the Intramural Research Program of the NIH (National Institute of Environmental Health Sciences).

References

1. Lacroix-Fralish ML, Mogil JS. Progress in genetic studies of pain and analgesia. *Annu Rev Pharmacol Toxicol.* 2009; 49:97–121. [PubMed: 18834308]
2. Surprenant A, Rassendren F, Kawashima E, North RA, Buell G. The cytolytic P2Z receptor for extracellular ATP identified as a P2X receptor (P2X7). *Science.* 1996; 272:735–738. [PubMed: 8614837]
3. Locovei S, Scemes E, Qiu F, Spray DC, Dahl G. Pannexin1 is part of the pore forming unit of the P2X7 receptor death complex. *FEBS Lett.* 2007; 581:483–488. [PubMed: 17240370]
4. Liao G, et al. *In silico* genetics: identification of a functional element regulating *H2-Ea* gene expression. *Science.* 2004; 306:690–695. [PubMed: 15499019]
5. Adriouch S, et al. A natural P451L mutation in the cytoplasmic domain impairs the function of the mouse P2X7 receptor. *J Immunol.* 2002; 169:4108–4112. [PubMed: 12370338]
6. Iglesias R, et al. P2X7 receptor-Pannexin 1 complex: pharmacology and signaling. *Am J Physiol Cell Physiol.* 2008; 295:C752–C760. [PubMed: 18596211]
7. Lariviere WR, et al. Heritability of nociception. III. Genetic relationships among commonly used assays of nociception and hypersensitivity. *Pain.* 2002; 97:75–86. [PubMed: 12031781]
8. Fuller SJ, Stokes L, Skarratt KK, Gu BJ, Wiley JS. Genetics of the P2X7 receptor and human disease. *Purinergic Signal.* 2009; 5:257–262. [PubMed: 19319666]
9. Bradley HJ, et al. Residues 155 and 348 contribute to the determination of P2X7 receptor function via distinct mechanisms revealed by single-nucleotide polymorphisms. *J Biol Chem.* 2011; 286:8176–8187. [PubMed: 21205829]
10. Stokes L, et al. Two haplotypes of the P2X7 receptor containing the Ala-348 to Thr polymorphism exhibit a gain-of-function effect and enhanced interleukin-1 β secretion. *FASEB J.* 2010; 24:2916–2927. [PubMed: 20360457]
11. Zaykin DV. Optimally weighted Z-test is a powerful method for combining probabilities in meta-analysis. *J Evol Biol.* 2011; 24:1836–1841. [PubMed: 21605215]

12. Chessell IP, et al. Disruption of the P2X₇ purinoceptor gene abolishes chronic inflammatory and neuropathic pain. *Pain*. 2005; 114:386–396. [PubMed: 15777864]
13. Clark AK, et al. P2X₇-dependent release of interleukin-1 β and nociception in the spinal cord following lipopolysaccharide. *J Neurosci*. 2010; 30:573–582. [PubMed: 20071520]
14. Honore P, et al. A-740003 [N-(1-{\{[(Cyanoimino)(5-quinolinylamino) methyl]amino\}-2,2-dimethylpropyl)-2-(3,4-dimethoxyphenyl)acetamide], a novel and selective P2X₇ receptor antagonist, dose-dependently reduces neuropathic pain in the rat. *J Pharmacol Exp Ther*. 2006; 319:1376–1385. [PubMed: 16982702]
15. McGaraughty S, et al. P2X₇-related modulation of pathological nociception in rats. *Neuroscience*. 2007; 146:1817–1828. [PubMed: 17478048]
16. Broom DC, et al. Characterization of N-(Adamantan-1-ylmethyl)-5-[(3R-aminopyrrolidin-1-yl)methyl]-2-chloro-benzamide, a P2X₇ antagonist in animal models of pain and inflammation. *J Pharmacol Exp Ther*. 2008; 327:620–633. [PubMed: 18772321]
17. Dell'Antonio G, Quattrini A, Dal Cin E, Fulgenzi A, Ferrero ME. Antinociceptive effect of a new P_{2Z}/P2X₇ antagonist, oxidized ATP, in arthritic rats. *Neurosci Lett*. 2002; 327:87–90. [PubMed: 12098642]
18. Jarvis MF. The neuron-glia purinergic receptor ensemble in chronic pain states. *Trends Neurosci*. 2010; 33:48–57. [PubMed: 19914722]
19. Pelegrin P, Surprenant A. The P2X₇ receptor–pannexin connection to dye uptake and IL-1 β release. *Purinergic Signal*. 2009; 5:129–137. [PubMed: 19212823]
20. Di Virgilio F. Liaisons dangereuses: P2X₇ and the inflammasome. *Trends Pharmacol Sci*. 2007; 28:465–472. [PubMed: 17692395]
21. Mogil JS, Chanda ML. The case for the inclusion of female subjects in basic science studies of pain. *Pain*. 2005; 117:1–5. [PubMed: 16098670]
22. Mogil JS, et al. Hypolocomotion, asymmetrically directed behaviors (licking, lifting, finching, and shaking) and dynamic weight bearing (gait) changes are not measures of neuropathic pain in mice. *Mol Pain*. 2010; 6:34. [PubMed: 20529328]
23. Chaplan SR, Bach FW, Pogrel JW, Chung JM, Yaksh TL. Quantitative assessment of tactile allodynia evoked by unilateral ligation of the fifth and sixth lumbar nerves in the rat. *J Neurosci Methods*. 1994; 53:55–63. [PubMed: 7990513]
24. Callahan BL, Gil ASC, Levesque A, Mogil JS. Modulation of mechanical and thermal nociceptive sensitivity in the laboratory mouse by behavioral state. *J Pain*. 2008; 9:174–184. [PubMed: 18088557]
25. Decosterd I, Woolf CJ. Spared nerve injury: an animal model of persistent peripheral neuropathic pain. *Pain*. 2000; 87:149–158. [PubMed: 10924808]
26. Shields SD, Eckert WA III, Basbaum AI. Spared nerve injury model of neuropathic pain in the mouse: a behavioral and anatomic analysis. *J Pain*. 2003; 4:465–470. [PubMed: 14622667]
27. Grupe A, et al. *In silico* mapping of complex disease-related traits in mice. *Science*. 2001; 292:1915–1918. [PubMed: 11397946]
28. Wang J, Liao G, Usuka J, Peltz G. Computational genetics: from mouse to human. *Trends Genet*. 2005; 21:526–532. [PubMed: 16009447]
29. Salter MW, Hicks JL. ATP causes release of intracellular Ca²⁺ via the phospholipase C β /IP₃ pathway in astrocytes from the dorsal spinal cord. *J Neurosci*. 1995; 15:2961–2971. [PubMed: 7722640]
30. Jiang LH, Mackenzie AB, North RA, Surprenant A. Brilliant Blue G selectively blocks ATP-gated rat P2X₇ receptors. *Mol Pharmacol*. 2000; 58:82–88. [PubMed: 10860929]

**Figure 1.**

Haplotype mapping of SNI-induced mechanical allodynia reveals a genetic association with the P451L variant of the mouse *P2rx7* gene. **(a)** The percentage of the maximum possible allodynia in 18 inbred mouse strains ($F_{17,82} = 2.3$, $P < 0.01$; one-way analysis of variance (ANOVA)). Data are mean \pm s.e.m. $n = 8$ –26 mice per strain. **(b)** Standardized (z -score) data ordered by strain from least allodynia (left) to most allodynia (right). Strains with the Pro451 allele are shown as black bars, and strains with the Leu451 allele are shown as white bars (the NZB/BN strain has the Leu451 allele). **(c)** The top five statistical associations (ranked by P value from the ANOVA model) genome wide between mechanical allodynia severity and 5,694 SNP haplotype blocks. The colored blocks represent the haplotypes of the 18 strains, listed from least allodynia (left) to most allodynia (right). The most common haplotype is shown in red, the second most common haplotype is shown in blue, and the third most common haplotype is shown in green. The genetic effect score represents the proportion of the observed interstrain phenotypic difference explained by the genetic variation within that haplotype block. The chromosomal (Chr.) position of the start of the haplotype block is given in Mb, as are the number of SNPs within the block. **(d–g)** Comparisons of all mice, grouped by P451L genotype (that is, carrying the Pro451 allele or the Leu451 allele). All data are mean \pm s.e.m. Baseline withdrawal thresholds **(d)**, ipsilateral mechanical allodynia **(e)**, contralateral allodynia (negative values represent hypoalgesia) **(f)** and ipsilateral allodynia (measured as the average percent change from baseline on postoperative days 5 and 7) **(g)** of an independently tested cohort of mice. Baseline was measured in noninjured mice, and allodynia was measured after SNI in each strain. $n = 8$ –26 mice per strain. * $P < 0.05$, ** $P < 0.01$, *** $P < 0.001$ compared to the opposite genotype, Student's t test.

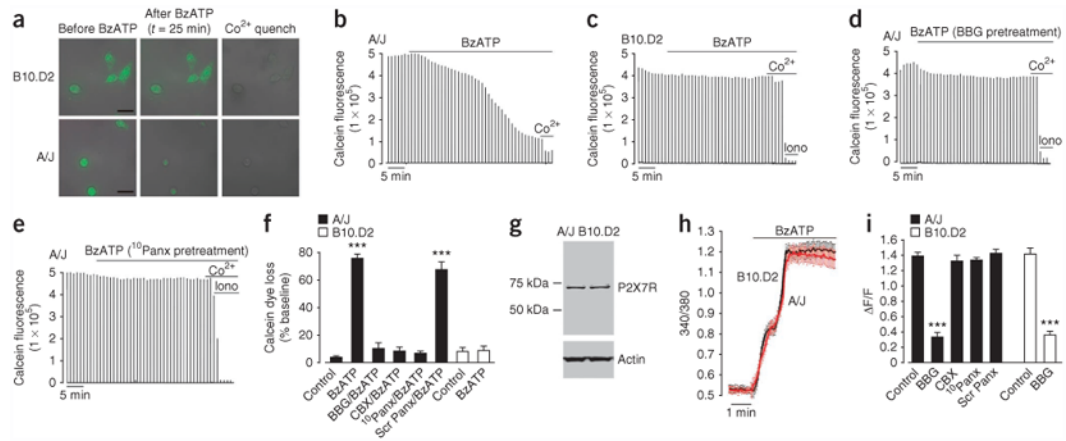


Figure 2.

BzATP causes calcein dye loss from the representative Pro451-carrying A/J mouse strain but not the Leu451-carrying B10.D2 mouse strain. (a-f) Peritoneal macrophages from A/J or B10.D2 mice were loaded with the dye calcein AM. (a) Photomicrographs of differential interference contrast or calcein fluorescence in A/J and B10.D2 macrophages. Scale bars, 25 μm. (b-e) Representative traces of calcein fluorescence, as measured by a photomultiplier detector. Cells were stimulated with the P2X7R agonist BzATP. Co²⁺ did not quench the calcein fluorescence in B10.D2 cells until after the addition of ionomycin (Iono). (d,e) Calcein fluorescence of A/J macrophages pretreated with the P2X7R antagonist BBG (d) or the pannexin 1 inhibitor ¹⁰Panx (e) before BzATP stimulation. (f) Calcein dye loss for control A/J macrophages, A/J macrophages with no pretreatment and A/J macrophages pretreated with BBG, carbenoxolone (CBX), ¹⁰Panx or the scrambled inactive version of ¹⁰Panx, scr Panx, before BzATP stimulation, as well as contro B10.D2 macrophages and B10.D2 macrophages stimulated with BzATP with no pretreatment. Data are mean ± s.e.m. (g) Western blot of P2X7R protein expression in whole-brain homogenates. (h) BzATP stimulation evoked a rise in intracellular [Ca²⁺] in A/J and B10.D2 macrophages loaded with the fluorescent Ca²⁺ indicator dye fura-2 AM. 340/380, the ratio of fluorescence at 340 nm to that at 380 nm. (i) The peak rise in intracellular [Ca²⁺] evoked by BzATP in cells loaded with fura-2 AM. ΔF/F represents the peak BzATP-evoked calcium response expressed relative to baseline. Data are mean ± s.e.m. *n* = 5-7 mice for each experimental group. ****P* < 0.001 compared to vehicle treated; ANOVA followed by Tukey's *post-hoc* test.

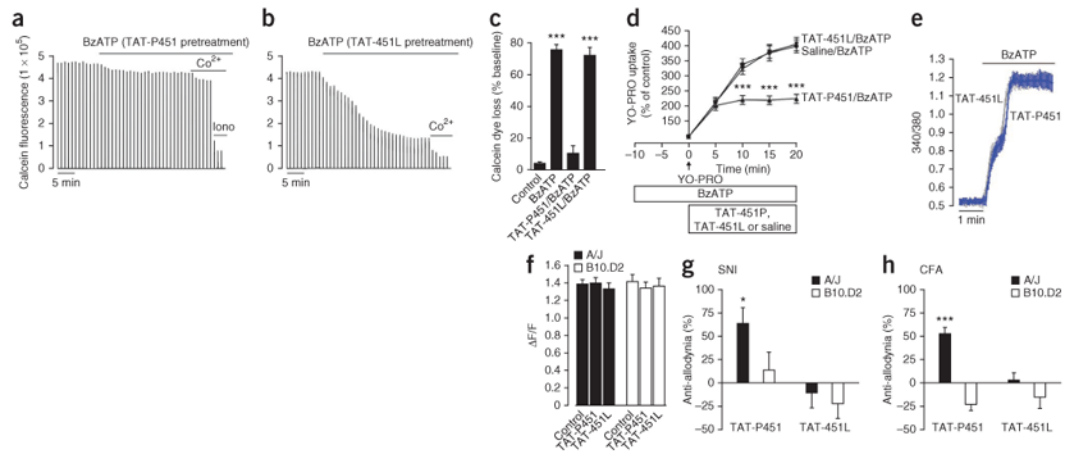


Figure 3.

Treatment with the TAT-P451 peptide prevents and reverses pore formation induced by BzATP and reverses the mechanical allodynia caused by peripheral nerve injury (SNI) or inflammation (CFA) in A/J mice. **(a,b)** Representative traces of calcein fluorescence of A/J macrophages treated with TAT-P451 or TAT-451L before BzATP stimulation. **(c)** Calcein dye loss in A/J macrophages treated as in **a** and **b**. Data are mean ± s.e.m. *** $P < 0.001$ compared to the control group; ANOVA followed by Tukey's *post-hoc* test. **(d)** YO-PRO uptake in cells treated with TAT-P451, TAT-451L or saline after 10 min BzATP stimulation. Data are mean ± s.e.m. *** $P < 0.001$ compared to saline; ANOVA followed by *t* test. **(e)** BzATP-evoked rise in intracellular [Ca²⁺] in fura-2 AM-loaded A/J macrophages pretreated with TAT-P451 or TAT-451L. **(f)** Peak rise in intracellular [Ca²⁺] evoked by BzATP in A/J and B10.D2 macrophages loaded with fura-2 AM and pretreated with TAT-P451 or TAT-451L. Data are mean ± s.e.m. For all *in vitro* experiments, each experimental group represents $n = 5-7$ mice. **(g,h)** Reversal of mechanical allodynia induced by nerve injury (SNI) **(g)** or inflammation (CFA) **(h)** by intravenous administration of TAT-P451 (but not TAT-451L) in A/J but not B10.D2 mice. Data are mean ± s.e.m. Anti-allodynia indicates reversal of allodynia. $n = 6-13$ mice per strain per peptide treatment group. * $P < 0.05$, *** $P < 0.001$ compared to all other groups; ANOVA followed by *t* test.

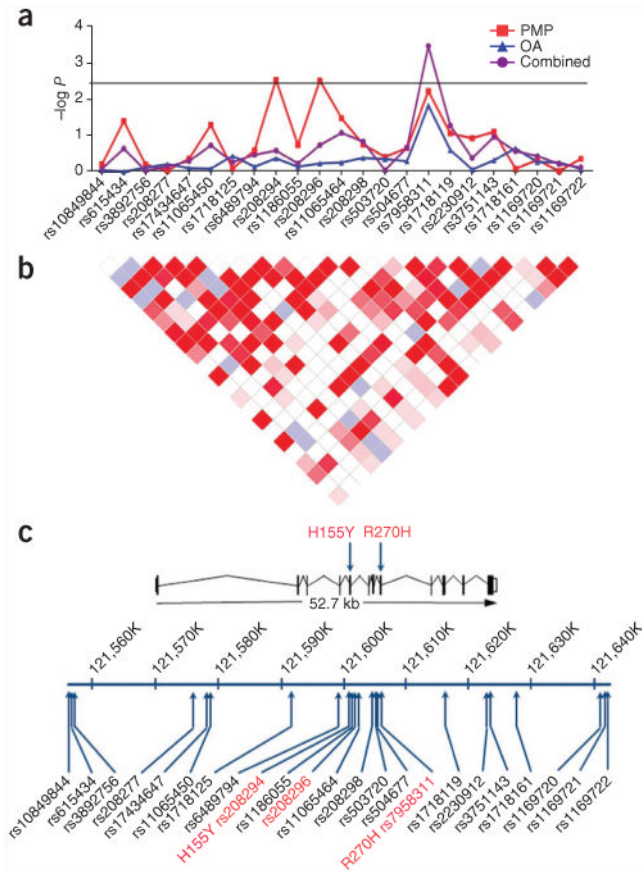


Figure 4.

Genetic association of the human *P2RX7* gene with chronic pain. (a) Significance of the association (expressed as $-\log P$) between 23 SNPs in and near the human *P2RX7* gene and the amount of chronic pain in two cohorts, the PMP and osteoarthritis (OA) cohorts. A third set of P values (purple) is shown for the combination of the first two P values, assessed by the optimally weighted z -test. The SNPs genotyped in both cohorts are ordered by genomic position. The horizontal line indicates the $P < 0.05$ significance threshold corrected for the number of effectively independent multiple comparisons after accounting for the linkage disequilibrium (LD) between the SNPs. (b) The LD between each pair of SNPs in terms of D' values: red indicates strong LD ($D' = 1$), with lighter shades of pink indicating decreasing LD. Blue and white indicate $D' = 1$ and $D' < 1$, respectively, with low confidence (by \log_{10} odds score) in the value of D' . No haplotype blocks (regions of widespread high LD) were observed among the SNPs. (c) The positions of the 23 genotyped SNPs in a 90.3-kb region containing the *P2RX7* gene. The intron and exon structure of the 52.7-kb gene itself is shown in the inset. SNPs with significant associations are shown in red.